

1 **Lytic bacteriophage vB_KmiS-Kmi2C disrupts biofilms formed by members of**
2 **the *Klebsiella oxytoca* complex, and represents a novel virus family and genus**

3

4 Fiona Newberry¹, Preetha Shibu^{2#}, Thomas Smith-Zaitlik¹, Mohamed Eladawy^{1,3},

5 Anne L. McCartney¹, Lesley Hoyles^{1*}, David Negus^{1*}

6

7 ¹ Department of Biosciences, Nottingham Trent University, United Kingdom

8 ² Life Sciences, University of Westminster, United Kingdom

9 ³ Microbiology and Immunology Department, Faculty of Pharmacy, Mansoura

10 University, Egypt

11

12 * **Corresponding authors:** David Negus, david.negus@ntu.ac.uk; Lesley Hoyles,

13 lesley.hoyles@ntu.ac.uk

14 # **Present address:** Berkshire and Surrey Pathology Services, Frimley Health NHS

15 Trust, Wexham Park Hospital, Slough, United Kingdom.

16

17 **Abbreviations:** CARD, comprehensive antibiotic resistance database; KoC,

18 *Klebsiella oxytoca* complex; PC, protein cluster; RBP, receptor binding protein; SD,

19 standard deviation; TEM, transmission electron microscopy; TSA, tryptone soy agar;

20 TSBG, tryptone soy broth supplemented with 1 % glucose; VC, viral cluster; VFDB,

21 virulence factor database.

22 **Keywords:** multidrug-resistant, *Klebsiella michiganensis*, siphovirus, phage

23 taxonomy, biofilm.

24 **Running headline:** *Klebsiella* phage vB_KmiS-Kmi2C.

25 **Data availability:** The genome sequence of vB_KmiS-Kmi2C has been deposited
26 with GenBank under accession OP495736. Updated genome data for *K.*
27 *michiganensis* strains PS_Koxy1, PS_Koxy2 and PS_Koxy4 are available from
28 BioProject PRJNA562720.

29 **ABSTRACT**

30 AIMS

31 This study aimed to characterise the lytic phage vB_KmiS-Kmi2C, isolated from
32 sewage water on a GES-positive strain of *Klebsiella michiganensis*.

33 METHODS AND RESULTS

34 Comparative phylogenetic and network-based analyses were used to characterise
35 the genome of phage vB_KmiS-Kmi2C (circular genome of 42,234 bp predicted to
36 encode 55 genes), demonstrating it shared little similarity with other known phages.
37 The phage was lytic on clinical strains of *K. oxytoca* (n=2) and *K. michiganensis*
38 (n=4), and was found to both prevent biofilm formation and disrupt established
39 biofilms produced by these strains.

40 CONCLUSIONS

41 We have identified a phage capable of killing clinically relevant members of the
42 *Klebsiella oxytoca* complex (KoC). The phage represents a novel virus family
43 (Dilsviridae) and genus (Dilsvirus).

44 SIGNIFICANCE AND IMPACT OF THE STUDY

45 Identification a novel lytic phage active against clinically relevant strains of the KoC
46 provides an alternative to antibiotics to treat these increasingly antimicrobial-resistant
47 opportunistic pathogens. The unusual way in which the phage can disrupt
48 established biofilms may allow us to identify novel phage-based approaches for
49 biofilm remediation in the future.

50

51 **INTRODUCTION**

52 Bacteriophages (phages) are viruses of bacteria that infect their bacterial
53 hosts for the purpose of replication. In the case of lytic phages, this process results
54 in lysis and destruction of the host. The potential for applying the bactericidal action
55 of lytic phages in a therapeutic setting was realised shortly after their discovery, with
56 d'Herelle performing the first recorded clinical studies in 1918 (d'Herelle, 1918).
57 Although interest in phage therapy diminished in Western countries following the
58 introduction of antibiotics, the emergence of multidrug-resistant pathogens has
59 resulted in a resurgence of interest.

60 Members of the *Klebsiella oxytoca* complex (KoC) are emerging as a serious
61 health concern. The complex currently consists of several distinct phylogroups,
62 representing *K. oxytoca* (Ko2), *K. michiganensis* (Ko1, Ko5), *K. grimontii* (Ko6), *K.*
63 *huaxiensis* (Ko8), *K. pasteurii* (Ko4), *K. spallanzanii* (Ko3), and three unnamed novel
64 species (Merla *et al.*, 2019; Yang *et al.*, 2022). Members are phylotyped based on
65 the sequence of their chromosomally encoded β -lactamase (*bla_{oxy}*) gene (Cosic *et*
66 *al.*, 2021). KoC bacteria can cause a range of serious infections in both humans and
67 animals and are of particular concern in healthcare settings where
68 immunocompromised patients are predisposed to potential infection. Isolates have
69 been associated with urinary tract infections, lower respiratory tract infections,
70 septicaemia, and soft-tissue injuries (Sohn, Seo & Jung, 2012; Paasch, Wilczek &
71 Strik, 2017; Shakya *et al.*, 2017; Lee *et al.*, 2019). Certain members of the complex
72 (*K. oxytoca*, *K. pasteurii*, *K. grimontii*, *K. michiganensis*) also encode the
73 kleboxymycin biosynthetic gene cluster associated with antibiotic-associated
74 haemorrhagic colitis (Shibu *et al.*, 2021). Worryingly, antibiotic resistance amongst

75 KoC members is increasing and resistance mechanisms include extended-spectrum
76 beta-lactamases and carbapenemases (Lowe *et al.*, 2012; White *et al.*, 2016).

77 New treatment options for tackling drug-resistant infections caused by KoC
78 isolates would be a welcome addition to our therapeutic armoury. This study aimed
79 to characterise the morphology, genome and host range of a lytic phage, vB_KmiS-
80 Kmi2C, isolated against a GES-5-encoding strain of *K. michiganensis* (PS_Koxy2)
81 (Shibu *et al.*, 2021). The anti-biofilm properties of the phage were investigated to
82 further determine therapeutic utility with respect to preventing or resolving biofouling
83 by KoC bacteria such as that which occurs on medical devices, particularly
84 indwelling catheters and ventilators. Further extensive genomic and phylogenetic
85 analyses of vB_KmiS-Kmi2C reveal that it represents a novel genus of phage.

86

87 **MATERIALS AND METHODS**

88 **Strain and cultivation information**

89 Details of all strains included in this study can be found in **Table 1**. All strains
90 were grown on nutrient agar (Sigma Aldrich) unless stated otherwise. Nutrient broth
91 (Sigma Aldrich) was used for overnight cultures unless stated otherwise, incubated
92 aerobically at 37 °C. All media used for phage assays were supplemented with
93 CaCl₂ and MgCl₂ (both at final concentration of 0.5 mM). The study of anonymised
94 clinical isolates provided by the Nottingham University Hospitals NHS Trust (NUH)
95 Pathogen Bank was approved by NUH Research and Innovation (19MI001).

96

97 **Generation of hybrid genome sequences**

98 Cell pellets from 10-ml overnight cultures grown in nutrient broth were sent to
99 microbesNG (Birmingham, UK) for DNA extraction, library preparation and

100 sequencing according to the sequencing provider's strain-submission procedures
101 (refer to
102 [https://microbesng.com/documents/24/MicrobesNG Sequencing Service Methods](https://microbesng.com/documents/24/MicrobesNG_Sequencing_Service_Methods_v20210419.pdf)
103 [v20210419.pdf](https://microbesng.com/documents/24/MicrobesNG_Sequencing_Service_Methods_v20210419.pdf) for the protocol).

104 For Illumina sequencing, the Nextera XT Library Preparation Kit (Illumina, San
105 Diego, USA) was used and paired-end reads (HiSeq/NovaSeq; 2x250 bp were
106 generated for PS_Koxy1 (coverage 141x), PS_Koxy2 (coverage 52x) and
107 PS_Koxy4 (coverage 57x). Reads were adapter-trimmed using Trimmomatic 0.30
108 (Bolger, Lohse & Usadel, 2014) with a sliding window quality cut-off of Q15. For
109 Illumina/MinION hybrid genomes, long-read genomic DNA libraries were prepared
110 with Oxford Nanopore SQK-RBK004 kit and/or SQK-LSK109 kit with Native
111 Barcoding EXP-NBD104/114 (ONT, United Kingdom) using 400–500 ng of high-
112 molecular-weight DNA. Barcoded samples were pooled together into a single
113 sequencing library and loaded into a FLO-MIN106 (R.9.4.1) flow cell in a GridION
114 (ONT, United Kingdom). *De novo* genome assembly was performed using Unicycler
115 v0.4.0 (Wick *et al.*, 2017).

116 The genome assemblies returned to us by microbesNG were annotated in-
117 house using Bakta v1.6.1, database v4.0 (Schwengers *et al.*, 2021). RGI 6.0.0,
118 CARD 3.2.5 was used to predict antimicrobial resistance genes encoded within
119 genomes (Alcock *et al.*, 2020). COPLA and plaSquid were used to characterise
120 plasmids harboured by strains (Redondo-Salvo *et al.*, 2021; Giménez, Ferrés &
121 Iraola, 2022).

122

123 **Biolog GEN III MicroPlate assays**

124 All strains were grown aerobically overnight on blood-free BUG agar (Biolog)
125 at 37 °C. For each assay, one to two colonies were used to inoculate Biolog
126 Inoculation Fluid B to a turbidity of 95 % (Biolog turbidimeter). Biolog Gen III plates
127 were inoculated according to the manufacturer's instructions, and incubated
128 aerobically at 37 °C for 22 h. Results were read at 540 nm using a BioTek Cytation]³
129 imaging reader spectrophotometer. All Biolog reagents and kits were purchased from
130 Technopath. Assays were carried out in triplicate for strains PS_Koxy1, PS_Koxy2
131 and PS_Koxy4.

132

133 **Biofilm assays and their interpretation**

134 Biofilm assays were performed as described previously (Stepanovic *et al.*,
135 2000; Merritt, Kadouri & O'Toole, 2005; Eladawy *et al.*, 2021). In brief, a single
136 colony of each strain was used to inoculate 5 ml of tryptone soy broth supplemented
137 with 1 % glucose (TSBG). Cultures were incubated aerobically for 24 h at 37 °C
138 without shaking. The overnight cultures were diluted to 1:100 using TSBG, then
139 aliquots (100 µl) of the diluted cultures were introduced into wells of a 96-well plate.
140 The plates were incubated aerobically for 24 h at 37 °C without shaking. Then, the
141 spent medium was carefully removed from each well. The wells were washed three
142 times with 200 µl sterile phosphate-buffered saline (pH 7.4; Oxoid) to remove any
143 non-adherent planktonic cells. The adherent cells were fixed by heat treatment at 60
144 °C for 60 min to prevent widespread detachment of biofilms prior to dye staining. The
145 adhered biofilms were then stained by addition of 1 % (w/v) crystal violet (150 µl per
146 well) and the 96-well plate was left to incubate for 20 min. The excess stain was then
147 carefully removed from the wells and discarded. The 96-well plate was then carefully
148 rinsed with distilled water three times, and the plate was inverted and left at room

149 temperature until the wells were dry. The stained biofilms were solubilised by adding
150 33 % (v/v) glacial acetic acid (Sigma Aldrich) to each well (150 µl per well). After
151 solubilisation of the stained biofilms, the OD₅₄₀ was measured and recorded for all
152 samples using a BioTek Cytation ³ imaging reader spectrophotometer. *K.*
153 *michiganensis* Ko14 and uninoculated medium were used as negative controls in
154 biofilm assays. Biological (*n*=3) and technical (*n*=4) replicates were done for all
155 strains. The mean of each isolate's OD quadruplicate readings (OD_{*i*}) was calculated
156 and compared with the control cut-off OD (OD_{*c*}), which was defined as three
157 standard deviations (SD) above the mean of the negative control (3SD + mean). The
158 amount of biofilm formed was scored as non-adherent (OD_{*i*} ≤ OD_{*c*}), weakly adherent
159 (OD_{*c*} < OD_{*i*} ≤ 2 OD_{*c*}), moderately adherent (2 OD_{*c*} < OD_{*i*} ≤ 4 OD_{*c*}) or strongly
160 adherent (4 OD_{*c*} < OD_{*i*}).

161

162 **Isolation of lytic phage and host range analysis**

163 Filter-sterilised sewage samples (0.45 µm cellulose acetate filter; Millipore)
164 collected from mixed-liquor tanks at Mogden Sewage Treatment Works (March
165 2017) were screened against *K. michiganensis* strain PS_Koxy2 as described
166 previously (Smith-Zaitlik *et al.*, 2022). Host range analysis was carried out as
167 described previously (Smith-Zaitlik *et al.*, 2022). After overnight incubation, overlay
168 assay plates were inspected for lysis, with results recorded according to a
169 modification of (Haines *et al.*, 2021): ++, complete lysis; +, hazy lysis; 0, no visible
170 plaques.

171

172 **Phage concentration and transmission electron microscopy (TEM)**

173 The Vivaspin 20 50 kDa centrifugal concentrator (Cytiva) was used to
174 concentrate filter-sterilised propagated phage as described previously (Smith-Zaitlik
175 *et al.*, 2022). For TEM, formvar/carbon-coated 200 mesh copper grids (Agar
176 Scientific) were prepared via glow discharge (10 mA, 10 s) using a Q150R ES
177 sputter coater (Quorum Technologies Ltd) and processed as described previously
178 (Smith-Zaitlik *et al.*, 2022). Samples were visualised using a JEOL JEM-2100Plus
179 (JEOL Ltd) TEM and an accelerating voltage of 200 kV. Images were analysed and
180 annotated using ImageJ (<https://imagej.net/Fiji>).

181

182 **Phage DNA extraction and sequencing**

183 Phage DNA was extracted from concentrated phage lysate using the Qiagen
184 DNeasy Blood & Tissue Kit as described previously (Smith-Zaitlik *et al.*, 2022).
185 Sequence data were generated on our in-house Illumina MiSeq platform, with the
186 Nextera XT DNA library preparation kit (Illumina) to produce fragments of
187 approximately 500 bp. Fragmented and indexed samples were run on the sequencer
188 using a Micro flow cell with the MiSeq Reagent Kit v2 (Illumina; 150-bp paired-end
189 reads) following Illumina's recommended denaturation and loading procedures.

190

191 **Phage genome assembly and annotation**

192 Quality of raw sequence data was assessed using [FastQC](#) v0.11.9. Reads
193 had a mean phred score above 30 and contained no adapter sequences, so data
194 were not trimmed. Genomes were assembled using SPAdes v3.15.4 (Bankevich *et*
195 *al.*, 2012) and visualised using Bandage v0.8.1 (Wick *et al.*, 2015). Contamination
196 and completeness of genomes were determined using CheckV v0.8.1 (CheckV
197 database v1.0) (Nayfach *et al.*, 2021). Gene annotations were made using Prokka

198 (v1.14.6) with the PHROGs database (v3) (Terzian *et al.*, 2021). Genomes were
199 screened for antimicrobial resistance genes using the Resistance Gene Identifier
200 (v5.2.0) of the Comprehensive Antibiotic Resistance Database (CARD) (v3.1.4)
201 (Alcock *et al.*, 2020), and for virulence genes using the Virulence Factor Database
202 (VFDB) (accessed: 6/6/2022) (Liu *et al.*, 2019). **Presence of temperature-lifestyle
203 genes was determined using PhageLeads (Yukgehnaish *et al.*, 2022).** An annotated
204 genome map was generated using GenoPlotR (v0.8.11) and predicted protein
205 function from the PHROGs database (Guy, Kultima & Andersson, 2010). **To identify
206 potential depolymerase-associated genes, predicted protein names were searched
207 for the following terms: 'depolymerase', 'pectin', 'pectate', 'sialidase', 'levanase',
208 'xylosidase', 'rhamnosidase', 'dextranase', 'alginate', 'hyaluronidase', 'hydrolase',
209 'lyase'.**

210

211 **Comparative genome analysis**

212 To generate a gene-sharing network, 21,903 phage genomes from the
213 INPHARED database (April 2022) and the query phage were clustered using
214 vConTACT2 (v0.9.22; default settings) and visualised in Cytoscape (v.3.9.1) (Bolduc
215 *et al.*, 2017; Cook *et al.*, 2021). The viral cluster (VC) containing the query phage
216 was determined and a proteomic phylogenetic tree generated from all phage within
217 the same VC using VipTree (v1.1.2; default settings) (Nishimura *et al.*, 2017).
218 *Klebsiella oxytoca* phage genomes vB_KmiM-2Dii (accession: MZ707156) and
219 vB_KmiM-4Dii (accession: MZ707157) were used as outliers. An additional
220 proteomic phylogenetic tree was generated from all phages within the VC and three
221 representative phage genomes from distantly related genera *Nonagvirus* (JenK1;
222 NC_029021.1), *Seuratvirus* (CaJan; NC_028776.1) and *Nipunavirus* (NP1;

223 NC_031058.1). The large terminase protein sequences were used to generate a
224 maximum likelihood phylogenetic tree with ClustalW (v.2.1) and IQTree with 1000
225 bootstraps (v1.6.12) (Thompson, Higgins & Gibson, 1994; Minh, Nguyen & von
226 Haeseler, 2013). IQModelFinder (v.1.4.2) was used with IQTree to determine the
227 model of best fit (Kalyaanamoorthy *et al.*, 2017). The percentage of shared proteins
228 within the VC was determined using all-versus-all BLASTP (≥ 30 % identity and ≥ 50
229 % sequence coverage; v2.12.0) (Turner, Kropinski & Adriaenssens, 2021). The
230 intergenomic similarity between phage within the same VC was determined using
231 VIRIDIC (v1.0) (Moraru, Varsani & Kropinski, 2020). ComplexHeatmap was used to
232 generated all heatmaps (Gu, Eils & Schlesner, 2016).

233

234 **Phage–biofilm assays**

235 The titre of the phage stock was determined by plaque assay using the
236 double-layer agar technique. Briefly, phage vB_KmiS-Kmi2C was serially diluted in
237 phosphate-buffered saline (pH 7.4; Oxoid) and 100 μ l of each phage dilution was
238 combined with 100 μ l of an overnight culture of *K. michiganensis* PS_Koxy2 and 5 ml
239 of 0.6 % tryptone soy agar (TSA) supplemented with CaCl₂ and MgCl₂ both at a final
240 concentration of 1 mM. The mixture was gently swirled and poured onto solid TSA
241 plates. Plates were incubated overnight at 37 °C and pfu/ml determined by
242 enumeration of visible plaques.

243 The ability of vB_KmiS-Kmi2C to prevent and disrupt biofilms was examined
244 using a modification of a previously described protocol (Taha *et al.*, 2018). Hosts of
245 vB_KmiS-Kmi2C identified as moderately ($2 OD_c < OD_i \leq 4 OD_c$) adherent were
246 included in the assay. For prevention of biofilms, host cultures were incubated
247 aerobically for 24 h at 37 °C without shaking in TSBG. Overnight cultures were

248 diluted 1:100 with TSBG and aliquots (100 µl) of diluted culture were introduced into
249 wells of a 96-well plate with or without phage vB_KmiS-Kmi2C (added to a final
250 concentration of 4.5×10^8 pfu/ml to each test well). Plates were incubated without
251 shaking for 24 h at 37 °C. Then, the supernatants were discarded, the biofilm of each
252 well was washed to remove planktonic cells and biofilms stained as described
253 above.

254 To investigate the disruption of established biofilms, host cultures were grown
255 and prepared as described above prior to inoculating a 96-well plate. Plates were
256 incubated without shaking for 24 h at 37 °C to allow biofilms to form. Unattached
257 planktonic cells were carefully aspirated without disrupting the biomass. Phage
258 vB_KmiS-Kmi2C diluted in 100 µl TSBG was added to test wells (final titre of 4.5×10^8
259 pfu/ml) whereas control wells received only TSBG without phage. Plates were
260 incubated for a further 24 h at 37 °C without shaking. Supernatants were carefully
261 discarded; the biofilm of each well was washed to remove planktonic cells and
262 biofilms stained as described above. Biological ($n=3$) and technical ($n=4$) replicates
263 were completed for all strains.

264

265

266

267 **RESULTS**

268 **Host range of phage vB_KmiS-Kmi2C**

269 Phage vB_KmiS-Kmi2C was isolated from sewage water on *K. michiganensis*
270 PS_Koxy2 (ST138), a multidrug-resistant, GES-5-positive isolate recovered from
271 human urine (Shibu *et al.*, 2021). The phage was screened against 56 clinical and 28
272 animal isolates representing a range of *Klebsiella* spp. (*K. michiganensis* n=49, *K.*
273 *oxytoca* n=25, *K. grimontii* n=9, *K. huaxiensis* n=1) (Shibu *et al.*, 2021; Smith-Zaitlik
274 *et al.*, 2022). It did not infect the closely related *K. michiganensis* strains PS_Koxy1
275 and PS_Koxy4 (Shibu *et al.*, 2021). vB_KmiS-Kmi2C did not infect animal isolates of
276 *Klebsiella* spp. (Smith-Zaitlik *et al.*, 2022), but did infect some of the clinical *K.*
277 *oxytoca* (n=2) and *K. michiganensis* (n=4) strains within our extended in-house
278 collection (Smith-Zaitlik *et al.*, 2022) (**Table 1**). From strain information provided by
279 the Pathogen Bank (EUCAST testing) all these strains were resistant to amoxicillin,
280 and sensitive to amikacin, ceftazidime, ceftazidime, ceftriaxone, cefuroxime,
281 ciprofloxacin, ertapenem, gentamicin, meropenem, piptazobactam and trimethoprim.
282 Strains Ko13, Ko22, Ko43 and Ko53 were sensitive to co-amoxiclav; Ko21 was
283 resistant to co-amoxiclav; no data were supplied for Ko37 and co-amoxiclav. Phage
284 vB_KmiS-Kmi2C did not exhibit depolymerase activity (i.e. it did not form haloes
285 around plaques) on any of the strains that it infected.

286

287 **Genotypic and phenotypic characterisation of the GES-positive strains**

288 Our previous work had shown PS_Koxy1, PS_Koxy2 and PS_Koxy4 to be
289 very similar based on the analysis of draft genome sequence data (Shibu *et al.*,
290 2021). In this study, we generated hybrid assemblies of their genomes (**Table 2**).

291 The initial description of the strains' draft genomes (Ellington *et al.*, 2019)
292 predicted they each harboured an identical IncQ 8,300-bp circular GES-5-positive
293 plasmid, confirmed in this study. PS_Koxy2 and PS_Koxy4 both carried an identical
294 76,870-bp circular plasmid (replication initiation protein domain Rep_3, replicon type
295 IncR). The 4,448-bp plasmid carried by all three strains shared high identity with
296 seven other plasmids, harboured by *Salmonella enterica*, *Enterobacter* spp. and *K.*
297 *michiganensis* (**Table 3**). A comparison (progressiveMauve, not shown) of the
298 sequence of pPSKoxy2_4 with those of the other 4,448-bp plasmids in **Table 3**
299 showed they shared 4,446 identical sites (99.98 % pairwise identity) across their
300 length. A PlasmidMLST search returned no hits for the plasmid sequence. It was
301 found to be PTU-E3 (score 96.97 %) by COPLA, exceeding the 90 % threshold to
302 validate the plasmid taxonomic unit assignment [16], and to belong to mobility group
303 MOB1 with a Col440I replicon type by plaSquid (Giménez *et al.*, 2022). The
304 plasmid was predicted by Bakta to encode six genes (MobA, MobC, two YgdI/YgdR
305 family lipoproteins, two hypothetical proteins), an origin of replication, *oriT* and a non-
306 coding RNAI (**Figure 1a**). UniProt BLASTP analyses showed MobA shared 55 %
307 identity (across 517 aa) with the DNA relaxase MbeA of *Escherichia coli* (reviewed
308 UniProt record P13658); MobC shared 63.6 % identity (across 115 aa) with the
309 mobilisation protein MbeC of *E. coli* (reviewed UniProt record P13657). The 39-aa
310 hypothetical protein was predicted by I-TASSER (Zhang, 2008) to be an alpha helix,
311 while the 122-aa hypothetical protein was found to include a transmembrane
312 segment (HHPRED, UniRef30 (Zimmermann *et al.*, 2018)) that had limited structural
313 homology with only the *Escherichia coli* signal transduction protein PmrD
314 (PDB:4HN7) and the Vps26 dimer region of a fungal vacuolar protein sorting-
315 associated protein (PDB:7BLQ).

316 PS_Koxy4 could be differentiated from PS_Koxy1 and PS_Koxy2 by
317 phenotypic traits determined using the Biolog GEN III system (**Table 4**). PS_Koxy1
318 and PS_Koxy2 were resistant to the tetracycline antibiotic minocycline; both were
319 predicted to encode the tetracycline efflux pump *tet(A)* on incompletely assembled
320 plasmids (contig_3 PS_Koxy1, predicted to be FIIK by PlasmidMLST; contig_2
321 PS_Koxy2, predicted to be IncA/C ST12 by PlasmidMLST), but this gene was absent
322 from the genome of PS_Koxy4, with the strain sensitive to minocycline (**Figure 1b**,
323 **Table 4**).
324

325 **Biofilm-forming ability of strains used in this study**

326 We determined the biofilm-forming ability of strains used in this study as
327 described previously (Taha *et al.*, 2018). Our results show a wide range of biofilm-
328 forming abilities among the strains (**Figure 2a**; **Supplementary Table 1**), yet there
329 was no difference in the virulence factor profiles of PS_Koxy1, PS_Koxy2 and
330 PS_Koxy4 according to a VFDB (Liu *et al.*, 2019) analysis (**Supplementary Table**
331 **2**). Strains *K. michiganensis* PS_Koxy1, *K. michiganensis* Ko13, *K. michiganensis*
332 Ko21 and *K. michiganensis* Ko22 were identified as weakly adherent ($OD_c < OD_i \leq 2$
333 OD_c). Strains *K. michiganensis* PS_Koxy2, *K. michiganensis* PS_Koxy4, *K. oxytoca*
334 Ko37, *K. oxytoca* Ko43 and *K. oxytoca* Ko53 were identified as moderately adherent
335 ($2 OD_c < OD_i \leq 4 OD_c$). *K. michiganensis* Ko14 was used as a non-adherent
336 negative control ($OD_i \leq OD_c$).
337

338 **Capacity of phage vB_KmiS-Kmi2C to prevent and disrupt biofilms**

339 Phage vB_KmiS-Kmi2C was found to be highly effective at both preventing
340 (**Figure 2b**) and disrupting (**Figure 2c**) biofilms formed by isolates identified as

341 susceptible to lysis. Presence of vB_KmiS-Kmi2C was found to reduce biofilm
342 formation for all strains included in the study. This reduction was found to be
343 significant ($P < 0.01$) for three of the isolates tested (PS_Koxy2, Ko37 and Ko53)
344 compared to no-phage controls. Addition of vB_KmiS-Kmi2C to pre-established
345 biofilms also resulted in biofilm disruption, seen as a reduction in measured biofilm
346 compared to non-phage-treated controls. Biofilm disruption was determined to be
347 significant ($P < 0.05$) for isolates PS_Koxy2 and Ko37 compared to non-phage
348 treated controls.

349

350 **Morphology of phage vB_KmiS-Kmi2C**

351 TEM showed vB_KmiS-Kmi2C to have a siphovirus-like morphology (**Figure**
352 **3**). It had a long, non-contractile tail. The capsid diameter was 59.6 nm (SD 2.3 nm),
353 the tail and baseplate were 157.8 nm in length (SD 5.1 nm), and the phage had a
354 total length of 218.11 nm (SD 4.8) ($n=3$ measurements).

355

356 **Genome of phage vB_KmiS-Kmi2C**

357 The genome of phage vB_KmiS-Kmi2C was assembled into a single contig,
358 with 100 % completeness according to CheckV (Nayfach *et al.*, 2021). Assembly of
359 the phage was confirmed using visualisation with Bandage (**Supplementary Figure**
360 **1**). It comprised 42,234 bp (816 × coverage) and was predicted to encode 55 genes
361 (upper panel **Figure 4**). The genome is arranged into functional modules as typically
362 seen in phage genomes: replication/regulation, viral structure, DNA packaging and
363 lysis. Interesting genomic features of the genome included a Sak4-like ssDNA
364 annealing protein with single-strand DNA-binding protein, a Cas4-domain
365 exonuclease, a holin and a Rz-like spanin.

366 Analysis using NCBI BLASTN showed the genome of vB_KmiS-Kmi2C
367 shared 85.6 % identity (80 % query coverage) with a phage metagenome-assembled
368 genome (accession OP072809) recovered from human faeces in Japan (Nishijima *et*
369 *al.*, 2022). Preliminary analysis of the genome sequence using the online version of
370 ViPTree suggested the phage was novel (not shown). Further support for this came
371 from genomic similarity analysis (**Supplementary Figure 2**) and analyses of
372 protein–protein network data using vConTACT (**Figure 5**). According to vConTACT,
373 vB_KmiS-Kmi2C **shared** a VC with 38 other known phage from a range of genera:
374 *Septimatrevirus* (n=24), *Lokivirus* (n=6), *Titanvirus* (n=4), *Pradovirus* (n=1),
375 *Kilunavirus* (n=1) and 2 unclassified genera. The VC did not contain any other phage
376 isolated using *Klebsiella* and the majority of phage had *Pseudomonas* as an
377 assigned host (**Figure 6**). The intergenomic similarity within the VC ranged from 100
378 % to 2 %, with the highest similarity noted between phage within the same genus
379 (**Supplementary Figure 2**). vB_KmiS-Km2iC showed the highest genomic similarity
380 (18.8 %) to *Septimatrevirus* vB_Pae-Kakheti25, a *Pseudomonas* phage. **The genera**
381 ***Titanvirus*, *Lokivirus*, *Septimatrevirus* do not currently belong to any recognised**
382 **phage family, whereas *Pradovirus* belongs to the *Autographiviridae*, which are**
383 **podovirus-like in terms of their morphology. Therefore, we suggest vB_KmiS-Kmi2C**
384 **does not belong to any currently recognised phage family.**

385 The vConTACT output was used to determine the shared protein clusters
386 (PCs) within the VC compared to phage vB_KmiS-Kmi2C (lower panel **Figure 4**). Of
387 the 53 PCs identified in vB_KmiS-Kmi2C, 14 were shared between all phage within
388 the VC (007793 Cas4-domain exonuclease ([KJBENDCP_00001](#)); 006166 DNA
389 helicase ([KJBENDCP_00002](#)); 006824 DNA polymerase processivity factor
390 ([KJBENDCP_00003](#)); 004149 DNA polymerase ([KJBENDCP_00004](#)); 005059 tail

391 length tape measure protein ([KJBENDCP_00011](#)); 005663 Neck1 protein
392 ([KJBENDCP_00012](#)); 005850 minor tail protein ([KJBENDCP_00015](#)); 008503 tail
393 terminator ([KJBENDCP_00016](#)); 005899 head-tail adaptor Ad1
394 ([KJBENDCP_00018](#)); 003930 head scaffolding protein ([KJBENDCP_00022](#));
395 002520 portal protein ([KJBENDCP_00023](#)); 005106 terminase large subunit
396 ([KJBENDCP_00024](#)); 007093 Sak4-like ssDNA annealing protein
397 ([KJBENDCP_00053](#)); 008553 ssDNA binding protein ([KJBENDCP_000154](#)). Seven
398 of the shared PCs were associated with viral structure and six were associated with
399 viral replication/regulation. vB_KmiS-Kmi2C shared the most PCs with *Erwinia*
400 phage AH03, including **most** of the viral structure genome module.

401 Protein-based phylogenetic analysis with VipTree showed phages within the
402 VC grouped according to the assigned genus, with vB_Kmi2S-Kmi2C not within the
403 defined genus groups ([Figure 6](#)). vB_KmiS-Kmi2C showed the closest relationship
404 to *Erwinia* phage AH03, as previously noted in the lower panel of **Figure 4**. A
405 representative species from three closely related genera were included in a further
406 protein-based phylogenetic analysis to determine if vB_KmiS-Kmi2C grouped with
407 genera outside the VC defined by vConTACT: *Nipunavirus* NP1 (NC_031058),
408 *Nonagavirus* JenK1 (NC_024146) and *Seuratvirus* Cajan (NC_028776)
409 (**Supplementary Figure 3**). Analysis of the shared protein percentage within the
410 viral cluster was consistent with the intergenomic similarity and protein phylogenetic
411 analysis (**Supplementary Figure 4**). The phage belonging to the same genera
412 shared the highest percentage of proteins. vB_KmiS-Kmi2C shared the highest
413 percentage of proteins with *Pseudomonas* phage *Septimatrevirus* KP1 and *Erwinia*
414 phage AH03. This confirmed that vB_KmiS-Kmi2C does not belong to any currently
415 defined genus of phage.

416 Given that vB_KmiS-Kmi2C represents a novel family, genus and species of
417 phage, we propose the following taxonomy: *Duplodnaviria* › *Heunggongvirae* ›
418 *Uroviricota* › *Caudoviricetes* › *Dilsviridae* › *Dilsvirus* › vB_KmiS-Kmi2C.

Commented [LH1]: Do we need to do anything else here?
E.g. for bacteria, you have to provide the etymology as well
as the novel names.

420 DISCUSSION

421 There has been a significant research effort into the investigation of phages
422 for the treatment of *K. pneumoniae* infections and we have recently authored an
423 extensive review on phages of *Klebsiella* spp. (Herridge *et al.*, 2020). However, there
424 are relatively few studies documenting the isolation and characterisation of lytic
425 phages against members of the KoC (Kęsik-Szeloch *et al.*, 2013; Townsend *et al.*,
426 2021; Smith-Zaitlik *et al.*, 2022), an emerging group of clinical and veterinary
427 pathogens with growing antibiotic resistance. As such, we set out to identify phages
428 with the capacity to lyse clinically relevant members of the KoC. We have previously
429 reported on the characterisation of two such phages with lytic activity against
430 numerous species within the KoC (Smith-Zaitlik *et al.*, 2022). Here, we report on the
431 characterisation of phage vB_KmiS-Kmi2C isolated against a carbapenem-resistant
432 isolate of *K. michiganensis* (PS_Koxy2) (Shibu *et al.*, 2021), for which we generated
433 a hybrid genome assembly and phenotypic data to allow it to be differentiated from
434 closely related strains (PS_Koxy1, PS_Koxy4) from our in-house collection.

435 There were clear differences in the biofilm-forming abilities of the three GES-5
436 -positive strains, yet all strains encoded the same virulence factors (**Supplementary**
437 **Table 2**). We did not compare protein sequences of the virulence factors across the
438 strains. It is acknowledged that our understanding of KoC phenotypes is poor (Yang
439 *et al.*, 2022), and our future work will look to address how differences in biofilm-

440 forming abilities of KoC members and their genetic differences contribute to survival
441 and potentially pathogenicity.

442 While the three strains all carried two small (4,448 and 8,300 bp) plasmids,
443 only PS_Koxy2 and PS_Koxy4 carried a 76,860-bp plasmid. This and the other
444 larger plasmids carried by the strains will be described elsewhere as part of ongoing
445 work. The 8,300-bp IncQ plasmid carried by the three strains has been described
446 elsewhere (Ellington *et al.*, 2019). While the 4,448-bp plasmid (mobility group
447 MOB1, replicon type Col440I) has been detected in a strain of *K. michiganensis*
448 previously (AbuOun *et al.*, 2021), it has not been described in detail. Based on its
449 gene content (specifically, MobA/MobC), we predict the plasmid to be conjugative
450 plasmid. The MobA and MobC functional homologues MbeA and MbeC,
451 respectively, are required for efficient mobilisation of the ColE1 plasmid (Varsaki *et*
452 *al.*, 2012).

453

454 **Host range analysis and anti-biofilm properties**

455 Understanding the lytic profile of any individual phage is important for its
456 potential deployment in a clinical setting, either in an isolated form or for inclusion in
457 a phage cocktail that may increase host range and potentially suppress phage
458 resistance (Yang *et al.*, 2020). Ordinarily, phage host range is narrow, sometimes
459 down to the strain level. In accordance with this, we found that vB_KmiS-Kmi2C
460 exhibits a relatively narrow host range, lysing six clinical isolates from the KoC out of
461 a panel of 84 isolates representing a range of clinical and animal *Klebsiella* spp.

462 To further characterise the therapeutic potential of vB_KmiS-Kmi2C,
463 experiments were performed to determine the phage's capacity to prevent and
464 disrupt biofilms formed by the clinical isolates susceptible to lysis in our host range

465 analysis. Biofilm formation can reduce the efficacy of antibiotic chemotherapy and
466 contributes to the successful colonisation of wounds and indwelling medical devices
467 (Wang *et al.*, 2020). Therefore, phages with anti-biofilm properties may make
468 particularly attractive therapeutics. We found that vB_KmiS-Kmi2C is highly effective
469 at both preventing biofilm formation and disrupting established biofilms. It is likely
470 that prevention of biofilm formation is largely due to the lytic action of the phage,
471 resulting in cell death and the prevention of biofilm formation. However, established
472 biofilms can be extremely recalcitrant to disruption. This is likely due to the complex
473 nature of mature biofilms which are typically composed of numerous
474 macromolecules including, polysaccharides, proteins, nucleic acids and
475 metabolically inactive cells (Chhibber, Nag & Bansal, 2013). Phage-mediated
476 disruption of *K. michiganensis* biofilms has been previously reported in the literature
477 (Ku *et al.*, 2021). The lytic phage KMI8 was shown to disrupt a
478 *K. michiganensis* mono-biofilm produced by a strain expressing the polysaccharide
479 capsule KL70 locus. It was hypothesised this antibiofilm activity was largely due to
480 the activity of a potential phage-associated depolymerase, identified as a putative
481 endosialidase encoded within the KMI8 genome. The antibiofilm effects of phages
482 against *K. oxytoca* have also been investigated (Townsend, Moat & Jameson, 2020).
483 A recent study showed that phages originally isolated against *K. pneumoniae* were
484 able to reduce the viability of *K. oxytoca* biofilms when added at the start of biofilm
485 formation. However, the same phages were unable to reduce the viability of
486 established *K. oxytoca* biofilms. Here, we found that vB_KmiS-Kmi2C is highly
487 effective at disrupting established biofilms formed by both *K. michiganensis* and *K.*
488 *oxytoca*. In the present study, we found no evidence of depolymerase activity
489 associated with vB_KmiS-Kmi2C. Plaques on susceptible host lawns did not show

490 evidence of haloes which are typically indicative of depolymerase activity.
491 Furthermore, our bioinformatic analysis did not identify any genes associated with
492 depolymerase activity. Studies are therefore ongoing to determine the mechanism of
493 biofilm disruption used by vB_KmiS-Kmi2C.

494

495 **Phage vB_KmiS-Kmi2C represents a new genus**

496 Whole-genome sequencing is important for the identification of features
497 relevant to phage therapy and for aiding taxonomic classification. Genomic analysis
498 using the resistance gene identifier tool available through the comprehensive
499 antibiotic resistance database did not identify the presence of known antimicrobial
500 resistance mechanisms within the genome of vB_KmiS-Kmi2C. The presence of
501 such genes would suggest the potential to transfer antibiotic resistance markers
502 between bacteria if vB_KmiS-Kmi2C were to be applied therapeutically in a
503 polymicrobial setting. **PhageLeads did not detect the presence of classical lysogeny**
504 **genes, suggesting vB_KmiS-Kmi2C is exclusively lytic.**

505 Initial genome sequence analysis of vB_KmiS-Kmi2C using BLASTN and
506 ViPTree suggested that our phage was novel, sharing little sequence similarity with
507 other deposited phage genomes. To aid with taxonomy, we employed the gene-
508 sharing network analysis tool vConTACT2. Phage taxonomic assignment using
509 whole genome gene-sharing profiles has been shown to be highly accurate; a recent
510 study showed that vConTACT2 produces near-identical replication of existing genus-
511 level viral taxonomy assignments from the International Committee on Taxonomy of
512 Viruses (ICTV) (Bin Jang *et al.*, 2019). Our analysis using vConTACT2 and the
513 INPHRARED database of phage genomes identified that vB_KmiS-Kmi2C shared a
514 VC with 38 other sequenced phages. The VC was polyphyletic, containing phage

515 from at least five different genera, suggesting that vB_KmiS-Km2iC did not group
516 with any existing genus. Recently published guidelines have suggested that for
517 genome-based phage taxonomy, assignment to taxonomic ranks should be based
518 on nucleotide sequence identity across entire genomes (Adriaenssens & Brister,
519 2017; Turner *et al.*, 2021). These guidelines suggest any two phages belong to the
520 same species if they are more than 95 % identical across their genome and belong
521 to the same genus if they are more than 70 % identical. We used VIRIDIC to
522 determine the intergenomic similarity between vB_KmiS-Kmi2C and the 38 other
523 phages identified within the VC. Our findings show that based on these criteria,
524 vB_KmiS-Kmi2C cannot be assigned to any current species or genus as it shares
525 only 18.8 % genomic similarity to *Septimatrevirus* vB_Pae-Kakheti25, a
526 *Pseudomonas* phage, the closest nucleotide sequence relative we could identify.

527 Most of the phages within the VC (21/38) were identified as infecting bacteria
528 belonging to the genus *Pseudomonas*. According to the GenBank accession details
529 associated with the genomes of these phages, they were all isolated-on strains of *P.*
530 *aeruginosa*. A preliminary screen of vB_KmiS-Kmi2C against a panel of 11 *P.*
531 *aeruginosa* isolates did not identify any lytic activity against members of this species
532 (data not shown).

533 In addition to identifying phages belonging to a VC, vConTACT2 can also
534 identify proteins shared by members within the VC. Our analysis found that 14
535 proteins were shared between all phages within the VC, of which seven were
536 associated with viral structure and six were associated with viral
537 replication/regulation. At least 35 of the phages within the VC are from genera with
538 siphovirus-like morphology. It is therefore unsurprising that phages within the cluster
539 share several proteins related to general structure/morphology.

540 Phage vB_KmiS-Kmi2C is the only member of the VC known to infect
541 members of the genus *Klebsiella*. Host-cell tropism is often determined by receptor-
542 binding proteins (RBPs) which mediate recognition and attachment to host cells
543 (Dams *et al.*, 2019). RBPs are typically identified as phage tail fibres or spikes
544 (Nobrega *et al.*, 2018). The genomic region of vB_KmiS-Kmi2C encoding
545 hypothetical tail fibre proteins can be seen in **Figure 4** and comprises proteins
546 088411, 095417, 028210, 033709, 031062 and 060189 ([KJBENDCP_00005 to](#)
547 [KJBENDCP_00010](#)). Unannotated proteins within this region were confirmed to
548 share homology with phage tail fibre proteins by HHPred analysis using an e-value
549 cut-off of $>10^{-5}$. The tail fibre proteins of vB_KmiS-Kmi2C are not widely present
550 within the VC and are typically shared by only one or two phages within the cluster.
551 This may explain the host tropism of vB_KmiS-Kmi2C compared to other members
552 of the VC but further experimentation will be required to determine this. Protein
553 005059 ([KJBENDCP_00011](#)) is a predicted tail length tape measure protein; such
554 proteins are involved in determining tail length and participate in DNA injection into
555 the host-cells and are not involved in host recognition (Mahony *et al.*, 2016).

556 Our additional protein-based phylogenetic analyses, including phages from
557 outside the VC, highlighted that vB_Kmi2S_Kmi2C does not group with any genera
558 included in the analyses and as such does not belong to any currently defined genus
559 of phage.

560 Phages are recognised as the most abundant biological entities on the planet
561 and exhibit extensive biological diversity (Hendrix, 2002). With an estimated 10^{31}
562 phage virions in the biosphere (Hatfull, 2015) and 14,244 complete phage genomes
563 sequenced as of 2021 (Cook *et al.*, 2021), it is clear we have characterised a
564 relatively small number of distinct phages. However, with the cost of genome

565 sequencing falling and the capacity to assemble phage genomes from metagenome
566 sequence data, it is likely that the number of novel phages identified will increase
567 rapidly. The classification of phages representing entirely novel genera or
568 families/sub-families poses a challenge for taxonomy, especially when new isolates
569 share little sequence similarity with previously characterised phages. Previously,
570 tailed phages were assigned to a family based on morphology, with the families
571 *Podoviridae*, *Myoviridae* and *Siphoviridae* belonging to the order *Caudovirales*.
572 However, the increase in available phage sequence data has shown that these
573 families are paraphyletic. It has, therefore, been suggested that they are abolished,
574 and that phage morphology should no longer play a role in classification (Turner *et*
575 *al.*, 2021). Based on recently updated guidelines for the classification of phage
576 based on nucleotide sequence identity, and subsequent protein based phylogenetic
577 analyses, we show here that phage vB_KmiS-Kmi2C represents a new genus.

578

579 **AUTHOR CONTRIBUTION STATEMENT**

580 Conceptualisation: FN, PS, LH, DN. Data curation: all authors. Formal
581 analysis: FN, TSZ, PS, ME, ALM, LH, DN. Funding acquisition: PS, ALM, LH.
582 Investigation: FN, TSZ, PS, ME, ALM, LH, DN. Methodology: FN, ME, LH, DN.
583 Resources: ALM, LH, DN. Supervision: ALM, LH, DN. Visualisation: FN, LH, DN.
584 Writing – original draft: FN, ME, LH, DN. Writing – reviewing and editing: all authors.

585

586 **ACKNOWLEDGEMENTS**

587 PS was in receipt of an IBMS Research Grant (project title "Isolation of lytic
588 bacteriophages active against antibiotic-resistant *Klebsiella pneumoniae*"). Imperial
589 Health Charity is thanked for contributing to registration fees for the Professional

590 Doctorate studies of PS. ME is supported by the Egyptian Government – Ministry of
591 Higher Education/Egyptian Cultural and Education Bureau. This work used
592 computing resources funded by the Research Contingency Fund of the Department
593 of Biosciences, Nottingham Trent University (NTU). TSZ completed this work as part
594 of an MRes degree at NTU.

595

596 REFERENCES

- 597 AbuOun, M., Jones, H., Stubberfield, E., Gilson, D., Shaw, L.P., Hubbard, A.T.M., Chau, K.K., Sebra, R.,
598 Peto, T.E.A., Crook, D.W., Read, D.S., Gweon, H.S., Walker, A.S., Stoesser, N., Smith, R.P.,
599 Anjum, M.F. and On Behalf Of The Rehab Consortium, null (2021) A genomic
600 epidemiological study shows that prevalence of antimicrobial resistance in Enterobacterales
601 is associated with the livestock host, as well as antimicrobial usage. *Microb Genomics*. **7**,
602 000630.
- 603 Adriaenssens, E. and Brister, J.R. (2017) How to Name and Classify Your Phage: An Informal Guide.
604 *Viruses*. **9**, E70.
- 605 Alcock, B.P., Raphenya, A.R., Lau, T.T.Y., Tsang, K.K., Bouchard, M., Edalatmand, A., Huynh, W.,
606 Nguyen, A.-L.V., Cheng, A.A., Liu, S., Min, S.Y., Miroshnichenko, A., Tran, H.-K., Werfalli, R.E.,
607 Nasir, J.A., Oloni, M., Speicher, D.J., Florescu, A., Singh, B., Faltyn, M., Hernandez-
608 Koutoucheva, A., Sharma, A.N., Bordeleau, E., Pawlowski, A.C., Zubyk, H.L., Dooley, D.,
609 Griffiths, E., Maguire, F., Winsor, G.L., Beiko, R.G., Brinkman, F.S.L., Hsiao, W.W.L.,
610 Domselaar, G.V. and McArthur, A.G. (2020) CARD 2020: antibiotic resistome surveillance
611 with the comprehensive antibiotic resistance database. *Nucleic Acids Res*. **48**, D517–D525.
- 612 Bankevich, A., Nurk, S., Antipov, D., Gurevich, A.A., Dvorkin, M., Kulikov, A.S., Lesin, V.M., Nikolenko,
613 S.I., Pham, S., Pribelski, A.D., Pyshkin, A.V., Sirotkin, A.V., Vyahhi, N., Tesler, G., Alekseyev,
614 M.A. and Pevzner, P.A. (2012) SPAdes: a new genome assembly algorithm and its
615 applications to single-cell sequencing. *J Comput Biol J Comput Mol Cell Biol*. **19**, 455–477.
- 616 Bin Jang, H., Bolduc, B., Zablocki, O., Kuhn, J.H., Roux, S., Adriaenssens, E.M., Brister, J.R., Kropinski,
617 A.M., Krupovic, M., Lavigne, R., Turner, D. and Sullivan, M.B. (2019) Taxonomic assignment
618 of uncultivated prokaryotic virus genomes is enabled by gene-sharing networks. *Nat*
619 *Biotechnol*. **37**, 632–639.
- 620 Bolduc, B., Jang, H.B., Doucier, G., You, Z.-Q., Roux, S. and Sullivan, M.B. (2017) vConTACT: an iVirus
621 tool to classify double-stranded DNA viruses that infect Archaea and Bacteria. *PeerJ*. **5**,
622 e3243.
- 623 Bolger, A.M., Lohse, M. and Usadel, B. (2014) Trimmomatic: a flexible trimmer for Illumina sequence
624 data. *Bioinforma Oxf Engl*. **30**, 2114–2120.
- 625 Chhibber, S., Nag, D. and Bansal, S. (2013) Inhibiting biofilm formation by *Klebsiella pneumoniae*
626 B5055 using an iron antagonizing molecule and a bacteriophage. *BMC Microbiol*. **13**, 174.

- 627 Clokie, M.R., Millard, A.D., Letarov, A.V. and Heaphy, S. (2011) Phages in nature. *Bacteriophage*. **1**,
628 31–45.
- 629 Cook, R., Brown, N., Redgwell, T., Rihtman, B., Barnes, M., Clokie, M., Stekel, D.J., Hobman, J., Jones,
630 M.A. and Millard, A. (2021) INfrastructure for a PHAge REference Database: Identification of
631 Large-Scale Biases in the Current Collection of Cultured Phage Genomes. *PHAGE*. **2**, 214–223.
- 632 Cosic, A., Leitner, E., Petternel, C., Galler, H., Reinthaler, F.F., Herzog-Obereder, K.A., Tatscher, E.,
633 Raffl, S., Feierl, G., Högenauer, C., Zechner, E.L. and Kienesberger, S. (2021) Variation in
634 Accessory Genes Within the *Klebsiella oxytoca* Species Complex Delineates Monophyletic
635 Members and Simplifies Coherent Genotyping. *Front Microbiol.* **12**, 692453.
- 636 Dams, D., Brøndsted, L., Drulis-Kawa, Z. and Briers, Y. (2019) Engineering of receptor-binding
637 proteins in bacteriophages and phage tail-like bacteriocins. *Biochem Soc Trans.* **47**, 449–460.
- 638 Eladawy, M., El-Mowafy, M., El-Sokkary, M.M.A. and Barwa, R. (2021) Antimicrobial resistance and
639 virulence characteristics in ERIC-PCR typed biofilm forming isolates of *P. aeruginosa*. *Microb*
640 *Pathog.* **158**, 105042.
- 641 Ellington, M.J., Davies, F., Jauneikaite, E., Hopkins, K.L., Turton, J.F., Adams, G., Pavlu, J., Innes, A.J.,
642 Eades, C., Brannigan, E.T., Findlay, J., White, L., Bolt, F., Kadhani, T., Chow, Y., Patel, B.,
643 Mookerjee, S., Otter, J.A., Sriskandan, S., Woodford, N. and Holmes, A. (2019) A multi-
644 species cluster of GES-5 carbapenemase producing Enterobacterales linked by a
645 geographically disseminated plasmid. *Clin Infect Dis Off Publ Infect Dis Soc Am.*
- 646 Giménez, M., Ferrés, I. and Iraola, G. (2022) Improved detection and classification of plasmids from
647 circularized and fragmented assemblies. *bioRxiv*.
- 648 Gu, Z., Eils, R. and Schlesner, M. (2016) Complex heatmaps reveal patterns and correlations in
649 multidimensional genomic data. *Bioinforma Oxf Engl.* **32**, 2847–2849.
- 650 Guy, L., Kultima, J.R. and Andersson, S.G.E. (2010) genoPlotR: comparative gene and genome
651 visualization in R. *Bioinforma Oxf Engl.* **26**, 2334–2335.
- 652 Haines, M.E.K., Hodges, F.E., Nale, J.Y., Mahony, J., van Sinderen, D., Kaczorowska, J., Alrashid, B.,
653 Akter, M., Brown, N., Sauvageau, D., Sicheritz-Pontén, T., Thanki, A.M., Millard, A.D., Galyov,
654 E.E. and Clokie, M.R.J. (2021) Analysis of Selection Methods to Develop Novel Phage Therapy
655 Cocktails Against Antimicrobial Resistant Clinical Isolates of Bacteria. *Front Microbiol.* **12**,
656 613529.
- 657 Hatfull, G.F. (2015) Dark Matter of the Biosphere: the Amazing World of Bacteriophage Diversity. *J*
658 *Viro.* **89**, 8107–8110.
- 659 Hendrix, R.W. (2002) Bacteriophages: Evolution of the Majority. *Theor Popul Biol.* **61**, 471–480.
- 660 d’Herelle, F. (1918) Sur le rôle du microbe filtrant bactériophage dans la dysentérie bacillaire.
661 *Comptes Rendus Académie Sci.* **167**, 970–972.
- 662 Herridge, W.P., Shibu, P., O’Shea, J., Brook, T.C. and Hoyles, L. (2020) Bacteriophages of *Klebsiella*
663 spp., their diversity and potential therapeutic uses. *J Med Microbiol.* **69**, 176–194.

- 664 Kalyaanamoorthy, S., Minh, B.Q., Wong, T.K.F., von Haeseler, A. and Jermini, L.S. (2017)
665 ModelFinder: fast model selection for accurate phylogenetic estimates. *Nat Methods*. **14**,
666 587–589.
- 667 Kęsik-Szeloch, A., Drulis-Kawa, Z., Weber-Dąbrowska, B., Kassner, J., Majkowska-Skrobek, G.,
668 Augustyniak, D., Łusiak-Szelachowska, M., Żaczek, M., Górski, A. and Kropinski, A.M. (2013)
669 Characterising the biology of novel lytic bacteriophages infecting multidrug resistant
670 *Klebsiella pneumoniae*. *Virology*. **10**, 100.
- 671 Ku, H., Kabwe, M., Chan, H.T., Stanton, C., Petrovski, S., Batinovic, S. and Tucci, J. (2021) Novel
672 Drexlerviridae bacteriophage KMI8 with specific lytic activity against *Klebsiella michiganensis*
673 and its biofilms. *PLoS ONE*. **16**, e0257102.
- 674 Lee, S.H., Ruan, S.-Y., Pan, S.-C., Lee, T.-F., Chien, J.-Y. and Hsueh, P.-R. (2019) Performance of a
675 multiplex PCR pneumonia panel for the identification of respiratory pathogens and the main
676 determinants of resistance from the lower respiratory tract specimens of adult patients in
677 intensive care units. *J Microbiol Immunol Infect*. **52**, 920–928.
- 678 Liu, B., Zheng, D., Jin, Q., Chen, L. and Yang, J. (2019) VFDB 2019: a comparative pathogenomic
679 platform with an interactive web interface. *Nucleic Acids Res*. **47**, D687–D692.
- 680 Lowe, C., Willey, B., O’Shaughnessy, A., Lee, W., Lum, M., Pike, K., Larocque, C., Dedier, H., Dales, L.,
681 Moore, C., McGeer, A., and the Mount Sinai Hospital Infection Control Team (2012)
682 Outbreak of Extended-Spectrum β -Lactamase-producing *Klebsiella oxytoca* Infections
683 Associated with Contaminated Handwashing Sinks. *Emerg Infect Dis*. **18**, 1242–1247.
- 684 Mahony, J., Alqarni, M., Stockdale, S., Spinelli, S., Feyereisen, M., Cambillau, C. and Sinderen, D. van
685 (2016) Functional and structural dissection of the tape measure protein of lactococcal phage
686 TP901-1. *Sci Rep*. **6**, 36667.
- 687 Merla, C., Rodrigues, C., Passet, V., Corbella, M., Thorpe, H.A., Kallonen, T.V.S., Zong, Z., Marone, P.,
688 Bandi, C., Sasser, D., Corander, J., Feil, E.J. and Brisse, S. (2019) Description of *Klebsiella*
689 *spallanzanii* sp. nov. and of *Klebsiella pasteurii* sp. nov. *Front Microbiol*. **10**, 2360.
- 690 Merritt, J.H., Kadouri, D.E. and O’Toole, G.A. (2005) Growing and analyzing static biofilms. *Curr*
691 *Protoc Microbiol*. **Chapter 1**, Unit 1B.1.
- 692 Minh, B.Q., Nguyen, M.A.T. and von Haeseler, A. (2013) Ultrafast Approximation for Phylogenetic
693 Bootstrap. *Mol Biol Evol*. **30**, 1188–1195.
- 694 Moraru, C., Varsani, A. and Kropinski, A.M. (2020) VIRIDIC—A Novel Tool to Calculate the
695 Intergenomic Similarities of Prokaryote-Infecting Viruses. *Viruses*. **12**, 1268.
- 696 Nayfach, S., Camargo, A.P., Schulz, F., Eloie-Fadrosch, E., Roux, S. and Kyrpides, N.C. (2021) CheckV
697 assesses the quality and completeness of metagenome-assembled viral genomes. *Nat*
698 *Biotechnol*. **39**, 578–585.
- 699 Nishijima, S., Nagata, N., Kiguchi, Y., Kojima, Y., Miyoshi-Akiyama, T., Kimura, M., Ohsugi, M., Ueki,
700 K., Oka, S., Mizokami, M., Itoi, T., Kawai, T., Uemura, N. and Hattori, M. (2022) Extensive gut
701 virome variation and its associations with host and environmental factors in a population-
702 level cohort. *Nat Commun*. **13**, 5252.

703 Nishimura, Y., Yoshida, T., Kuronishi, M., Uehara, H., Ogata, H. and Goto, S. (2017) ViPTree: the viral
704 proteomic tree server. *Bioinforma Oxf Engl.* **33**, 2379–2380.

705 Nobrega, F.L., Vlot, M., de Jonge, P.A., Dreesens, L.L., Beaumont, H.J.E., Lavigne, R., Dutilh, B.E. and
706 Brouns, S.J.J. (2018) Targeting mechanisms of tailed bacteriophages. *Nat Rev Microbiol.* **16**,
707 760–773.

708 Paasch, C., Wilczek, S. and Strik, M.W. (2017) Liver abscess and sepsis caused by *Clostridium*
709 *perfringens* and *Klebsiella oxytoca*. *Int J Surg Case Rep.* **41**, 180–183.

710 Redondo-Salvo, S., Bartomeus-Peñalver, R., Vielva, L., Tagg, K.A., Webb, H.E., Fernández-López, R.
711 and de la Cruz, F. (2021) COPLA, a taxonomic classifier of plasmids. *BMC Bioinformatics.* **22**,
712 390.

713 Schwengers, O., Jelonek, L., Dieckmann, M.A., Beyvers, S., Blom, J. and Goesmann, A. (2021) Bakta:
714 rapid and standardized annotation of bacterial genomes via alignment-free sequence
715 identification. *Microb Genomics.* **7**.

716 Shakya, P., Shrestha, D., Maharjan, E., Sharma, V.K. and Paudyal, R. (2017) ESBL Production Among *E.*
717 *coli* and *Klebsiella* spp. Causing Urinary Tract Infection: A Hospital Based Study. *Open*
718 *Microbiol J.* **11**, 23–30.

719 Shibu, P., McCuaig, F., McCartney, A.L., Kujawska, M., Hall, L.J. and Hoyles, L. (2021) Improved
720 molecular characterization of the *Klebsiella oxytoca* complex reveals the prevalence of the
721 kleboxymycin biosynthetic gene cluster. *Microb Genomics.* **7**, 000592.

722 Smith-Zaitlik, T., Shibu, P., McCartney, A.L., Foster, G., Hoyles, L. and Negus, D. (2022) Extended
723 genomic analyses of the broad-host-range phages vB_KmiM-2Di and vB_KmiM-4Dii reveal
724 slopekviruses have highly conserved genomes. *Microbiology.* **168**, 001247.

725 Sohn, W.-I., Seo, B.F. and Jung, S.-N. (2012) Forehead Abscess Caused by *Klebsiella oxytoca* With
726 Undiagnosed Type 2 Diabetes: *J Craniofac Surg.* **23**, 247–249.

727 Stepanovic, S., Vukovic, D., Dakic, I., Savic, B. and Svabic-Vlahovic, M. (2000) A modified microtiter-
728 plate test for quantification of staphylococcal biofilm formation. *J Microbiol Methods.* **40**,
729 175–179.

730 Taha, O.A., Connerton, P.L., Connerton, I.F. and El-Shibiny, A. (2018) Bacteriophage ZCKP1: A
731 Potential Treatment for *Klebsiella pneumoniae* Isolated From Diabetic Foot Patients. *Front*
732 *Microbiol.* **9**, 2127.

733 Terzian, P., Olo Ndela, E., Galiez, C., Lossouarn, J., Pérez Bucio, R.E., Mom, R., Toussaint, A., Petit, M.-
734 A. and Enault, F. (2021) PHROG: families of prokaryotic virus proteins clustered using remote
735 homology. *NAR Genomics Bioinforma.* **3**, lqab067.

736 Thompson, J.D., Higgins, D.G. and Gibson, T.J. (1994) CLUSTAL W: improving the sensitivity of
737 progressive multiple sequence alignment through sequence weighting, position-specific gap
738 penalties and weight matrix choice. *Nucleic Acids Res.* **22**, 4673–4680.

739 Townsend, E.M., Kelly, L., Gannon, L., Muscatt, G., Dunstan, R., Michniewski, S., Sapkota, H.,
740 Kiljunen, S.J., Kolsi, A., Skurnik, M., Lithgow, T., Millard, A.D. and Jameson, E. (2021) Isolation
741 and Characterization of *Klebsiella* Phages for Phage Therapy. *PHAGE.* **2**, 26–42.

742 Townsend, E.M., Moat, J. and Jameson, E. (2020) CAUTI's next top model - Model dependent
743 Klebsiella biofilm inhibition by bacteriophages and antimicrobials. *Biofilm*. **2**, 100038.

744 Turner, D., Kropinski, A.M. and Adriaenssens, E.M. (2021) A Roadmap for Genome-Based Phage
745 Taxonomy. *Viruses*. **13**, 506.

746 Varsaki, A., Lamb, H.K., Eleftheriadou, O., Vandera, E., Thompson, P., Moncalián, G., de la Cruz, F.,
747 Hawkins, A.R. and Drainas, C. (2012) Interaction between relaxase MbeA and accessory
748 protein MbeC of the conjugally mobilizable plasmid ColE1. *FEBS Lett*. **586**, 675–679.

749 Wang, G., Zhao, G., Chao, X., Xie, L. and Wang, H. (2020) The Characteristic of Virulence, Biofilm and
750 Antibiotic Resistance of Klebsiella pneumoniae. *Int J Environ Res Public Health*. **17**, 6278.

751 Webb, H.E., Kim, J.Y., Tagg, K.A., de la Cruz, F., Peñil-Celis, A., Tolar, B., Ellison, Z., Schwensohn, C.,
752 Brandenburg, J., Nichols, M. and Folster, J.P. (n.d.) Genome Sequences of 18 Salmonella
753 enterica Serotype Hadar Strains Collected from Patients in the United States. *Microbiol
754 Resour Announc*. **11**, e00522-22.

755 White, L., Hopkins, K.L., Meunier, D., Perry, C.L., Pike, R., Wilkinson, P., Pickup, R.W., Cheesbrough, J.
756 and Woodford, N. (2016) Carbapenemase-producing *Enterobacteriaceae* in hospital
757 wastewater: a reservoir that may be unrelated to clinical isolates. *J Hosp Infect*. **93**, 145–151.

758 Wick, R.R., Judd, L.M., Gorrie, C.L. and Holt, K.E. (2017) Unicycler: Resolving bacterial genome
759 assemblies from short and long sequencing reads. *PLoS Comput Biol*. **13**, e1005595.

760 Wick, R.R., Schultz, M.B., Zobel, J. and Holt, K.E. (2015) Bandage: interactive visualization of de novo
761 genome assemblies. *Bioinforma Oxf Engl*. **31**, 3350–3352.

762 Yachison, C.A., Yoshida, C., Robertson, J., Nash, J.H.E., Kruczkiewicz, P., Taboada, E.N., Walker, M.,
763 Reimer, A., Christianson, S., Nichani, A., PulseNet Canada Steering Committee and Nadon, C.
764 (2017) The Validation and Implications of Using Whole Genome Sequencing as a
765 Replacement for Traditional Serotyping for a National Salmonella Reference Laboratory.
766 *Front Microbiol*. **8**, 1044.

767 Yang, J., Long, H., Hu, Y., Feng, Y., McNally, A. and Zong, Z. (2022) Klebsiella oxytoca Complex:
768 Update on Taxonomy, Antimicrobial Resistance, and Virulence. *Clin Microbiol Rev*. **35**,
769 e0000621.

770 Yang, Y., Shen, W., Zhong, Q., Chen, Q., He, X., Baker, J.L., Xiong, K., Jin, X., Wang, J., Hu, F. and Le, S.
771 (2020) Development of a Bacteriophage Cocktail to Constrain the Emergence of Phage-
772 Resistant *Pseudomonas aeruginosa*. *Front Microbiol*. **11**, 327.

773 Yukgehnash, K., Rajandas, H., Parimannan, S., Manickam, R., Marimuthu, K., Petersen, B., Clokie,
774 M.R.J., Millard, A. and Sicheritz-Pontén, T. (2022) PhageLeads: Rapid Assessment of Phage
775 Therapeutic Suitability Using an Ensemble Machine Learning Approach. *Viruses*. **14**, 342.

776 Zhang, Y. (2008) I-TASSER server for protein 3D structure prediction. *BMC Bioinformatics*. **9**, 40.

777 Zimmermann, L., Stephens, A., Nam, S.-Z., Rau, D., Kübler, J., Lozajic, M., Gabler, F., Söding, J., Lupas,
778 A.N. and Alva, V. (2018) A Completely Reimplemented MPI Bioinformatics Toolkit with a
779 New HHpred Server at its Core. *J Mol Biol*. **430**, 2237–2243.

780

781 **Table 1.** *K. oxytoca* complex strains used in this study

Strain *	Species	Source	Reference
PS_Koxy1	<i>K. michiganensis</i>	Throat swab	(Shibu <i>et al.</i> , 2021)
PS_Koxy2 §#	<i>K. michiganensis</i>	Urine	(Shibu <i>et al.</i> , 2021)
PS_Koxy4	<i>K. michiganensis</i>	Rectal swab	(Shibu <i>et al.</i> , 2021)
Ko13 §	<i>K. michiganensis</i>	Blood culture	(Smith-Zaitlik <i>et al.</i> , 2022)
Ko14	<i>K. michiganensis</i>	Blood culture	(Smith-Zaitlik <i>et al.</i> , 2022)
Ko21 §	<i>K. michiganensis</i>	Perfusion fluid	(Smith-Zaitlik <i>et al.</i> , 2022)
Ko22 §	<i>K. michiganensis</i>	Perfusion fluid	(Smith-Zaitlik <i>et al.</i> , 2022)
Ko37 §	<i>K. oxytoca</i>	Blood culture	(Smith-Zaitlik <i>et al.</i> , 2022)
Ko43 §	<i>K. michiganensis</i>	Bile fluid	(Smith-Zaitlik <i>et al.</i> , 2022)
Ko53 §	<i>K. oxytoca</i>	Blood culture	(Smith-Zaitlik <i>et al.</i> , 2022)

782 * Ko prefix indicates strains came from the Pathogen Bank of Queen's Medical

783 Centre Nottingham, UK.

784 § Infected by phage vB_KmiS-Kmi2C.

785 # Strain on which phage vB_KmiS-Kmi2C was isolated; all other strains used in host

786 range analysis but not infected by the phage are described in (Smith-Zaitlik *et al.*,

787 2022).

788 **Table 2.** Summary statistics for hybrid genome assemblies of the GES-5-positive
 789 strains

Strain (accession)	Contigs	Size (bp)	Status *	N50	CDS	Plasmids (RIP; MOB; REP; PTU) #
PS_Koxy1 (GCA_014050555.2)	7	6,392,093	CCC; 4 CCPs; ? incomplete plasmid	6,023,296	5,952	pPSKoxy1_1 (RepA_C; MOBH; IncAC, IncN; -) pPSKoxy1_2 (Rep_3; -, IncR; -) pPSKoxy1_3 [-; MOBP1; -, PTU-Q2 (IncQ)] pPSKoxy1_4 (-; MOBP1; Col440; PTU-E3)
PS_Koxy2 (GCA_014050535.2)	10	6,357,486	Draft chromosome; 4 CCPs; ? incomplete plasmid	5,917,750	5,910	pPSKoxy2_1 (IncFII_repA, IncFII_repA, RepA_C, RepB-RCR_reg; MOBF, MOBH; IncFII_1_pKP91, IncAC, IncN; -) pPSKoxy2_2 (Rep_3; -, IncR; -) pPSKoxy2_3 [-; MOBP1; -, PTU-Q2 (IncQ)] pPSKoxy2_4 (-; MOBP1; Col440; PTU-E3)
PS_Koxy4 (GCA_014050515.2)	6	6,406,207	CCC; 5 CCPs	6,075,855	5,969	pPSKoxy4_1 (IncFII_repA, IncFII_repA, RepB- RCR_reg; MOBF; IncFII_1_pKP91; PTU-FK (IncFII)) pPSKoxy4_2 [-; MOBH; IncAC; PTU-C (IncA)] pPSKoxy4_3 (Rep_3; -, IncR; -) pPSKoxy4_4 [-; MOBP1; -, PTU-Q2 (IncQ)] pPSKoxy4_5 (-; MOBP1; Col440; PTU-E3)

Formatted: Italian (Italy)

Formatted: Italian (Italy)

Formatted: French (France)

Formatted: Italian (Italy)

790 *CCC, complete circular chromosome; CCP, complete circular plasmid.

791 # RIP, replication initiation protein domain; MOB, mobility group; REP, replicon type;

792 PTU, plasmid taxonomy unit; -, no data available. RIP, MOB and REP determined

793 using plaSquid (Giménez *et al.*, 2022), PTU determined using COPLA (Redondo-

794 Salvo *et al.*, 2021).

795

796 **Table 3.** Closest relatives of the circular 4,448 bp plasmid as determined using NCBI BLASTN

Species, strain and plasmid	Identity	Size (nt)	Accession	Source	Location	Reference
<i>S. enterica</i> PNUSAS021403 pPNUSAS021403_3	3511/3513 (99 %)	4,448	CP093106.1	Patient	USA	(Webb <i>et al.</i> , 2022)
<i>S. enterica</i> subsp. <i>enterica</i> serovar Hadar PNUSAS018090 pPNUSAS018090_3	2662/2664 (99 %)	4,448	CP093099.1	Patient	USA	(Webb <i>et al.</i> , 2022)
<i>S. enterica</i> 2016K-0377 p2016K-0377_3	4387/4389 (99 %)	4,448	CP093079.1	Patient	USA	(Webb <i>et al.</i> , 2022)
<i>S. enterica</i> subsp. <i>enterica</i> serovar Hadar 12-2388 p12-2388.3	2662/2664 (99 %)	4,448	CP038598.1	Reference laboratory	Canada	(Yachison <i>et al.</i> , 2017)
<i>E. cloacae</i> 78 pP6	3403/3403 (100 %)	9,923	OW849463.1	Hospital	Spain	BioProject PRJEB42440
<i>E. hormaechei</i> RHBSTW-00070 pRHBSTW-00070_3	3403/3403 (100 %)	9,923	CP058166.1	Wastewater influent	UK	(AbuOun <i>et al.</i> , 2021)
<i>K. michiganensis</i> RHBSTW-00676 pRHBSTW-00676_6	3211/3211 (100 %)	4,448	CP055990.1	Wastewater influent	UK	(AbuOun <i>et al.</i> , 2021)

Formatted: Spanish (Spain, Traditional Sort)

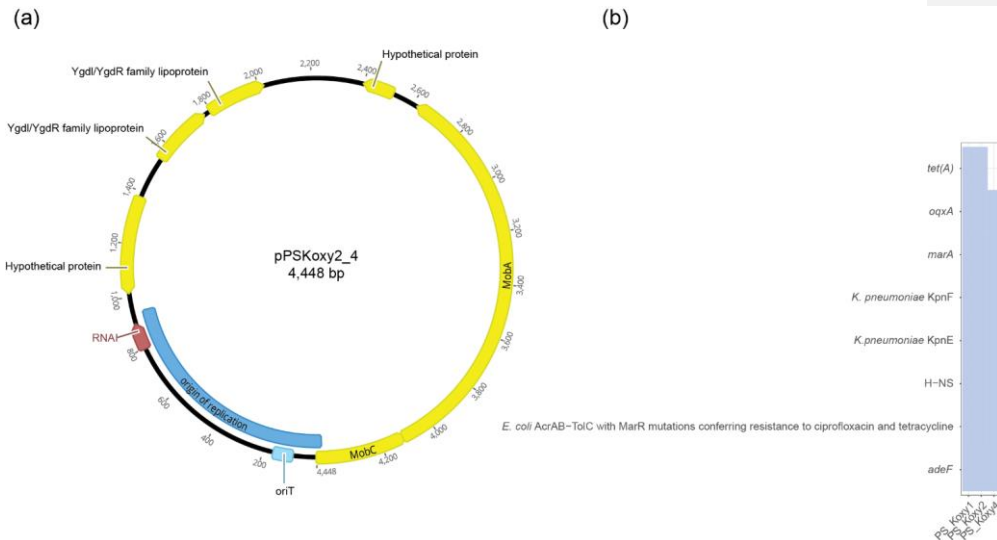
797

798 **Table 4.** Phenotypic traits that differentiate PS_Koxy1 and PS_Koxy2 from
799 PS_Koxy4

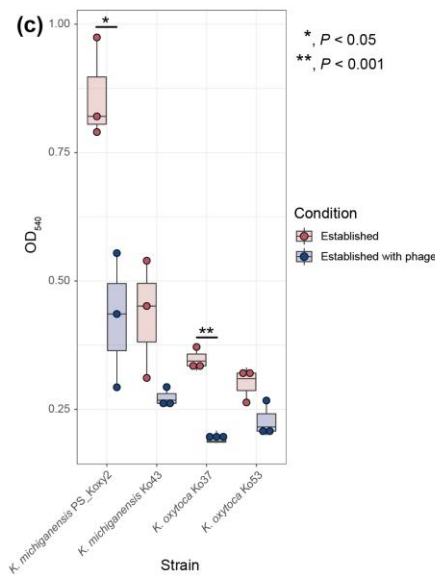
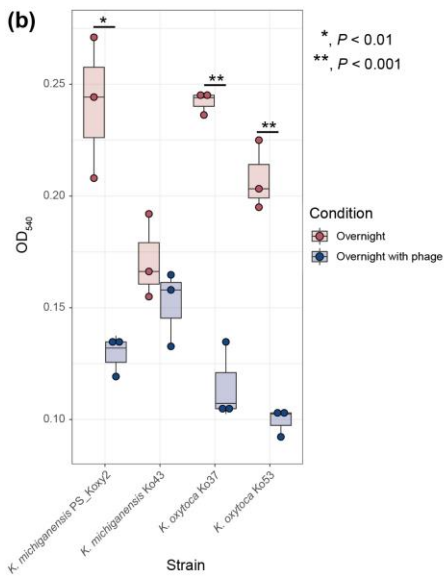
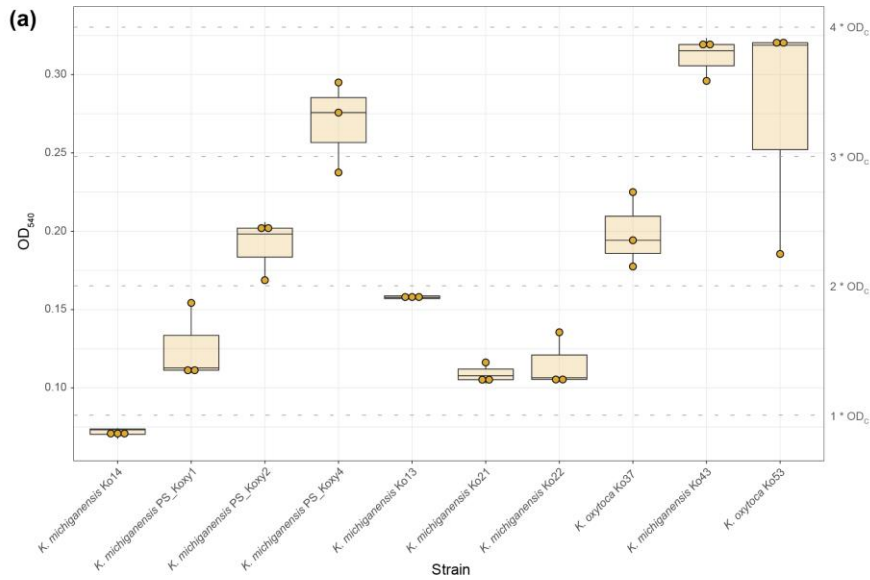
Growth in presence of	PS_Koxy1	PS_Koxy2	PS_Koxy4
D-Serine	-	-	+
L-Alanine	+	+	-
Minocycline	+	+	-
Acetic acid	-	-	+

800 +, Positive according to the Biolog GEN III system; -, negative according to the
801 Biolog GEN III system.

802



803
 804 **Figure 1. (a)** Illustration of the circular conjugative 4,448-bp plasmid harboured by *K.*
 805 *michiganensis* strains PS_Koxy1, PS_Koxy2 and PS_Koxy4. **(b)** Tetracycline-
 806 antibiotic-associated genes predicted to be encoded within the genomes of strains
 807 PS_Koxy1, PS_Koxy2 and PS_Koxy4 by RGI/CARD. All hits were considered 'strict'
 808 by CARD.
 809



810
 811 **Figure 2.** Biofilm-forming abilities of the strains used in this study. **(a)** The biofilm-
 812 forming abilities of all strains listed in **Table 1** were assessed. *K. michiganensis*
 813 Ko14, a strain that does not form biofilms in TSBG, was used as the negative
 814 control. Differences in biofilm formation in comparison with the control were

815 statistically significant for all strains (unpaired *t* test, adjusted *P* value < 0.05,
816 Benjamini-Hochberg; **Supplementary Table 1**). The ability of phage vB_KmiS-
817 Kmi2C to **(b)** prevent biofilm formation or **(c)** disrupt established biofilms was
818 assessed using those strains infected by the phage and forming the strongest
819 biofilms **(a)**. **(b, c)** Statistical significance of the differences in biofilm formation of
820 strains in the presence and absence of phage was assessed using unpaired *t* test.
821 **(a–c)** Data are shown as mean for four technical and three biological replicates per
822 strain.



823

824 **Figure 3.** Transmission electron micrograph of phage vB_KmiS-Kmi2C. Scale bar,

825 50 nm.

827 **Figure 4.** Genome map and predicted function of vB_KmiS-Kmi2C (upper image) and presence/absence of PCs within VC (lower
828 image). The genome map shows the predicted function of the coding regions, direction of transcription and PC ID for each gene
829 segment. The phage genus and host genus are shown to the left of the PC heatmap (see legend for annotation) and phage
830 genome size on the right-hand side of the heatmap.

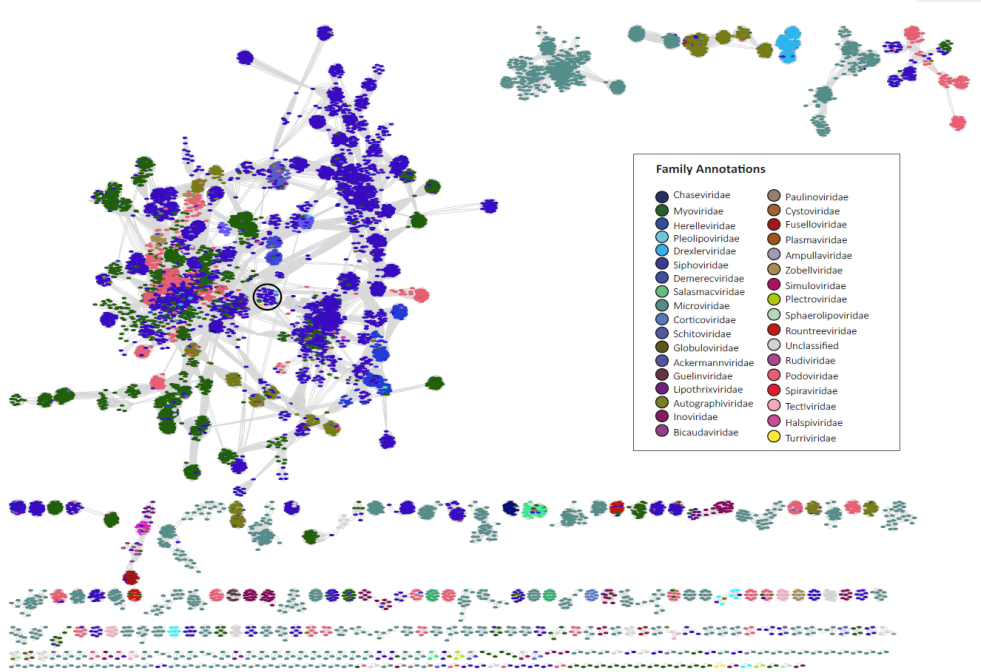


Figure 5. Protein-sharing network generated from vB_KmiS-Kmi2C and INPHARED database. Each node represents a phage genome and connection between the genomes shown by a grey line. The nodes are annotated according to viral family. The VC containing vB_KmiS-Kmi2C is highlighted with a black circle.

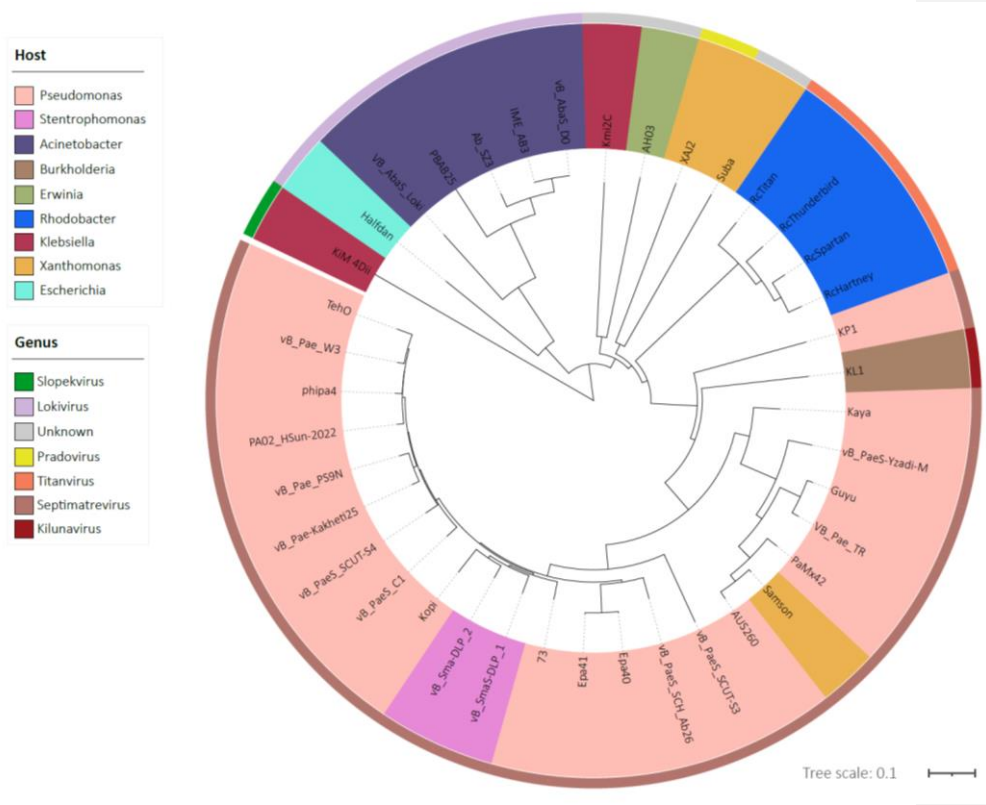


Figure 6. Protein phylogenetic analysis generated with VipTree from all phage within the VC. The inner circle is coloured according to phage host and outer circle according to assigned phage genus. The tree was rooted at the midpoint and scale shown in the bottom right. *Klebsiella* phage vB_KmiM-4Dii (KiM 4Dii), a *Slopekvirus* phage (Smith-Zaitlik *et al.*, 2022), was used as an outlier.